

Improved TaN barrier layer against Cu diffusion by formation of an amorphous layer using plasma treatment

Keng-Liang Ou, Wen-Fa Wu, Chang-Pin Chou, Shi-Yung Chiou, and Chi-Chang Wu

Citation: *Journal of Vacuum Science & Technology B* **20**, 2154 (2002); doi: 10.1116/1.1511214

View online: <http://dx.doi.org/10.1116/1.1511214>

View Table of Contents: <http://scitation.aip.org/content/avs/journal/jvstb/20/5?ver=pdfcov>

Published by the AVS: Science & Technology of Materials, Interfaces, and Processing

Articles you may be interested in

[Influence of N₂O plasma treatment on microstructure and thermal stability of WN_x barriers for Cu interconnection](#)

J. Vac. Sci. Technol. B **22**, 993 (2004); 10.1116/1.1715087

[Ta metallization of Si–O–C substrate and Cu metallization of Ta/Si–O–C multilayer](#)

J. Vac. Sci. Technol. B **21**, 293 (2003); 10.1116/1.1541606

[TaC as a diffusion barrier between Si and Cu](#)

J. Appl. Phys. **91**, 5391 (2002); 10.1063/1.1464652

[Diffusion barrier and electrical characteristics of a self-aligned MgO layer obtained from a Cu\(Mg\) alloy film](#)

Appl. Phys. Lett. **77**, 2192 (2000); 10.1063/1.1314879

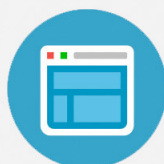
[Nanostructured Ta–Si–N diffusion barriers for Cu metallization](#)

J. Appl. Phys. **82**, 4847 (1997); 10.1063/1.366346



Re-register for Table of Content Alerts

Create a profile.



Sign up today!



Improved TaN barrier layer against Cu diffusion by formation of an amorphous layer using plasma treatment

Keng-Liang Ou

Institute and Department of Mechanical Engineering, National Chiao-Tung University, Hsinchu 300, Taiwan, Republic of China

Wen-Fa Wu^{a)}

National Nano Device Laboratories, Hsinchu 300, Taiwan, Republic of China

Chang-Pin Chou

Institute and Department of Mechanical Engineering, National Chiao-Tung University, Hsinchu 300, Taiwan, Republic of China

Shi-Yung Chiou

Department of Mold and Die Engineering, National Kaohsiung University of Applied Science, Kaohsiung 807, Taiwan, Republic of China

Chi-Chang Wu

National Nano Device Laboratories, Hsinchu 300, Taiwan, Republic of China

(Received 18 April 2002; accepted 12 August 2002)

The thermal stability and electrical properties of plasma-treated TaN films have been investigated by Cu/TaN/Si systems. The properties of diffusion barrier were evaluated by sheet resistance, x-ray diffraction (XRD), transmission electron microscopy (TEM), x-ray photoelectron spectroscopy (XPS), energy-dispersive spectroscopy (EDS), Auger electron microscopy (AES), and reverse-biased junction leakage current. A new amorphous layer is found to form on the surface of TaN film after the plasma treatment. Plasma-treated TaN films show better barrier performance than untreated TaN films. The sheet resistance of Cu/TaN(10 nm)/Si increases apparently after annealing at 625 °C for 1 h, while the Cu/plasma-treated TaN(10 nm)/Si is fairly stable up to annealing at 750 °C. The resistance to copper diffusion in plasma-treated TaN film is more effective. This is attributed that an amorphous layer that forms on the surface of TaN film after the plasma treatment. The thermal stabilities of Cu/TaN/ n^+ - p junction diodes are enhanced by plasma treatment. The Cu/TaN(10 nm)/ n^+ - p and Cu/TaN(50 nm)/ n^+ - p junction diodes result in large reverse-biased junction leakage currents after annealing at 525 and 575 °C, respectively. On the other hand, plasma-treated TaN diffusion barriers improve the integrity of junction diodes up to 650 °C. Nano crystallization and stuffing effects of plasma treatments are believed to impede Cu diffusion into the Si substrate and hence improve the barrier performance. © 2002 American Vacuum Society.

[DOI: 10.1116/1.1511214]

I. INTRODUCTION

As device dimensions become small towards 180 nm and below, interconnects will continue to be critical limitations for improving the performance and reducing costs of integrated circuits. Fundamental changes in existing interconnection materials can increase the maximum circuit speed. Cu whose resistance is 40% lower than Al is now being introduced into manufacturing. However, Cu atoms can diffuse into Si devices, and degrade the device performance by introducing a deep level acceptor.¹ Typical dielectric materials used in interconnects are not effective barriers to Cu diffusion. In addition, Cu has poor adhesion to them. Hence, Cu interconnects are required to have both an adhesion promoter and a diffusion barrier. The microstructure of the thin-film barrier can strongly affect the texture and grain size of deposited Cu. The preferred orientation and grain size of cop-

per are critical factors in determining electromigration reliability.² Thus, the thin barrier film is necessary to possess superior properties as mentioned above. Several diffusion barriers for Cu metallization have been investigated such as TiN,³ WN,⁴ Ta,^{5,6} and TaN.^{5,6} Unfortunately, most of these barriers are polycrystalline and provide inadequate protection because grain boundaries may presumably serve as fast diffusion paths for copper. Among these materials, Ta-N alloys are considered to be the most promising diffusion barriers for preventing Cu diffusion. Alloying Ta with N and /or O not only restricts the copper diffusion because of decoration of the extended defects, but also results in films with smaller grains and amorphous-like nanostructure.⁷

The purpose of the present investigation is twofold. The first is to prepare a thermally stable, ultrathin barrier layer between Cu and Si. TaN is selected as the barrier material in the present study because Ta has a low formation enthalpy (ΔH) with nitrogen and TaN has a high melting point of 3087 °C as well as a dense structure.⁸ Second, a method of forming nitrogen and oxygen incorporated TaN films is in-

^{a)}Author to whom correspondence should be addressed; electronic mail: wfwu@ndl.gov.tw

investigated. N_2 and O_2 plasmas are used to posttreat the tantalum nitride diffusion barriers. Properties of barrier layers are evaluated by electrical measurements and material analyses.

II. EXPERIMENTAL DETAILS

The substrates used in the present work were *p*-type (100) oriented silicon wafers with resistivity of 5–10 $\mu\Omega$ cm. The Si wafers were cleaned in a dilute HF solution (HF: H_2O = 1: 20) for 2 min, and rinsed in de-ionized water prior to loading into the sputtering system. The 10 nm TaN films were deposited at a power of 500 W and a sputtering pressure of 6.4 mTorr (0.85 Pa) after the base pressure was evacuated to below 5×10^{-7} Torr (6.67×10^{-5} Pa). The films were prepared using optimum conditions as in our previous investigations, and thus provided a more effective barrier capability against Cu diffusion.⁵ Some wafers further received *ex situ* nitrogen or oxygen plasma treatments in a plasma enhanced chemical vapor deposition system after tantalum nitride films were deposited. For easy identification, the untreated tantalum nitride, and nitrogen and oxygen plasma treated tantalum nitride films were denoted as TaN, TaN(N)/TaN, and TaN(O)/TaN, respectively. Copper films 300 nm thick were then deposited on top of the barrier layers by sputtering. Cu/TaN/Si, Cu/TaN(N)/TaN/Si, and Cu/TaN(O)/TaN/Si were annealed in N_2 ambient from 500 to 800 °C for 1 h to evaluate the thermal stability.

In order to analyze the properties of TaN-based barrier layers, x-ray photoelectron spectroscopy (XPS) using monochromatized Mg $K\alpha$ radiation was performed to identify the chemical states of TaN films with plasma treatments. The microstructure and film thickness were examined using transmission electron microscopy (TEM). Sheet resistance was measured by a four-point probe system. Film resistivity was derived from the sheet resistance and film thickness. Surface morphology of annealed Cu/barrier/Si was observed by scanning electron microscopy (SEM). Compositions of failure sites were analyzed by energy dispersive spectrometry (EDS) after removing both copper and barrier layers by wet-chemical solution. Grazing incidence x-ray diffractometry was carried out for phase identification. The incident angle of x ray was fixed at 3°. Auger electron microscopy (AES) was used to analyze the compositional depth profile after annealing. Cu/barrier/ n^+ -*p* junction diodes with conventional localized oxidation of silicon isolation were fabricated for electrical analyses. The diode leakage current was measured by a HP4145B semiconductor parameter analyzer at a reverse bias of -5 V after annealing at various temperatures for 1 h.

III. RESULTS AND DISCUSSION

A. Properties of plasma-treated TaN films

Figure 1 shows the glancing incidence x-ray diffraction spectra of 10 nm TaN films with N_2 or O_2 plasma treatments. The time shown in the parenthesis is the time of the plasma treatment. The intensity and shape of reflections indicate

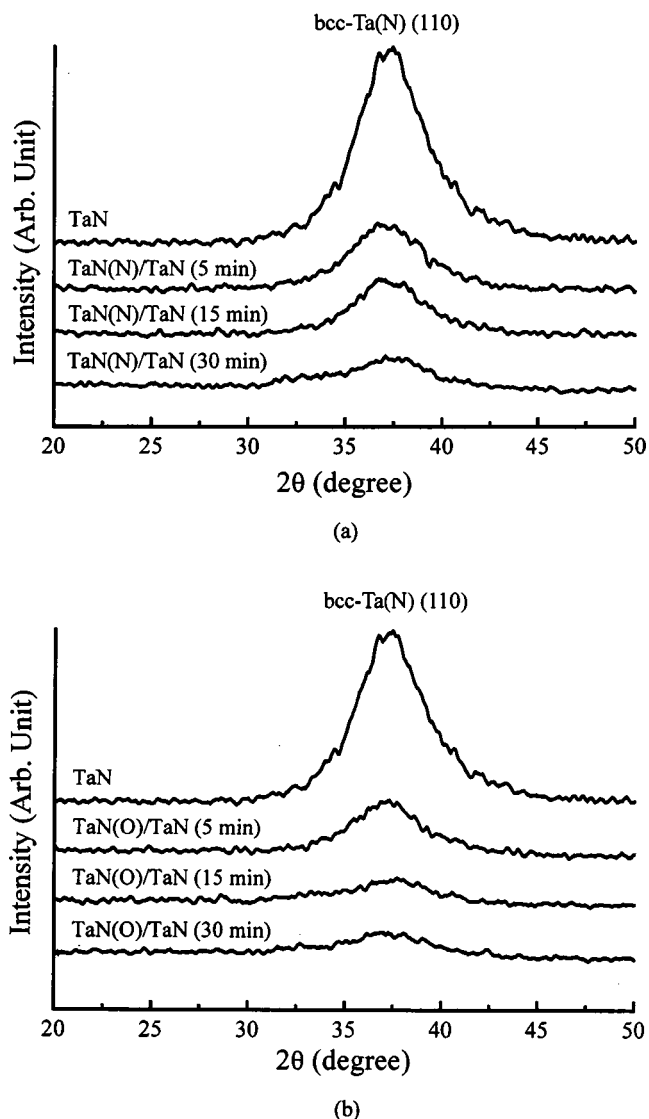
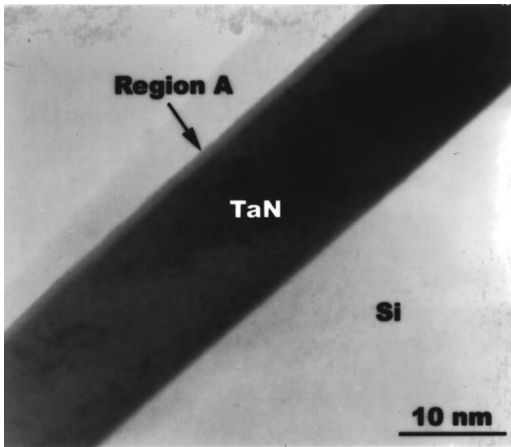
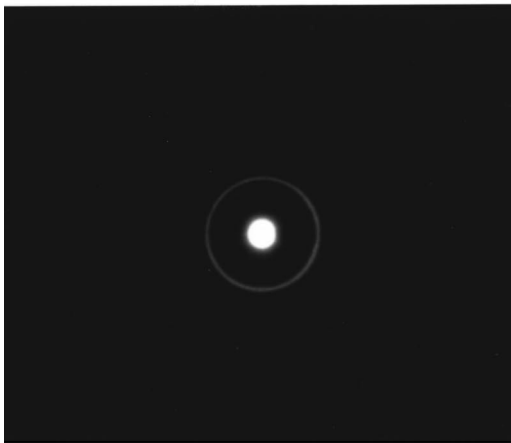


Fig. 1. XRD spectra of untreated and plasma-treated TaN(10 nm) films. (a) N_2 plasma. (b) O_2 plasma.

changes in the phase of the TaN film. As-deposited TaN films grow predominantly in bcc-Ta(N) phase and are apparently polycrystalline as determined by XRD analyses. With 5 min N_2 plasma treatment, the XRD peak is considerably broadened, as shown in Fig. 1(a). It implies that the plasma treatment leads to a microstructural modification of the TaN barrier layer. With increasing N_2 plasma treatment, the enhanced broadening of the peak is observed. Similar broadening results are found on TaN films with O_2 plasma treatments, as shown in Fig. 1(b). Figure 2 displays cross-sectional TEM micrograph and selected area diffraction pattern of 30 min O_2 plasma-treated TaN/Si (TaN(O)/TaN/Si). Multilayered structure is observed for the TaN film with O_2 plasma treatment as indicated in Fig. 2(a). Figure 2(b) demonstrates the selected area diffraction pattern taken from the region A. The electron diffraction pattern shows that the region A has a diffused ring pattern instead of diffraction spots. This indicates that the layer denoted as region A is an amorphous layer. Based on the above investigations, the development of an amorphous layer on the film surface is



(a)



(b)

FIG. 2. (a) Cross-sectional TEM micrograph of 30 min O₂ plasma-treated TaN/Si. (b) Selected area diffraction pattern in region A.

clearly observed after properly inducing plasma treatment. Figure 3 shows the selected area diffraction pattern of sputtered TaN film. Several sharp rings are observed for untreated TaN film. It indicates that as-deposited TaN film is a

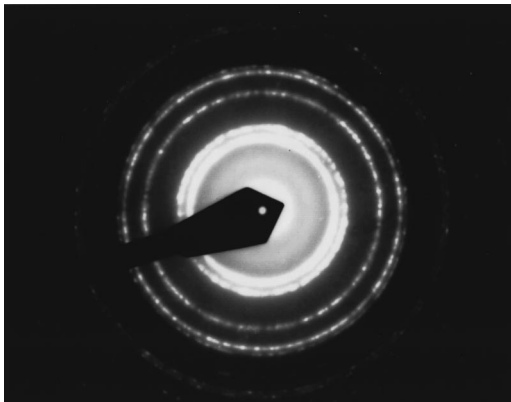


FIG. 3. Selected area diffraction pattern of untreated TaN film.

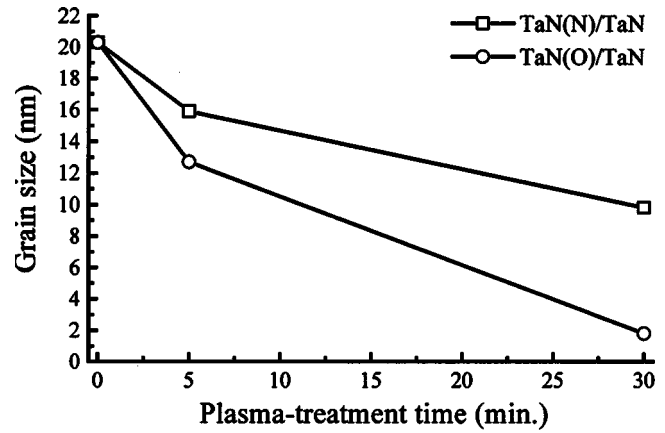


FIG. 4. Grain size of TaN(N)/TaN and TaN(O)/TaN films as a function of plasma treatment time.

polycrystalline structure. Figure 4 shows the grain size of TaN(N)/TaN and TaN(O)/TaN layers as a function of plasma treatment time. The grain size is calculated from plane-view TEM. The as-deposited TaN film is a polycrystalline structure with a grain size of ~20 nm. The grain size decreases with increasing plasma treatment time. It indicates that nano-crystallization effect would occur due to the reactions and bombardments of energetic radicals and ions during plasma treatment. Moreover, it is found that grain size of the TaN(O)/TaN film decreases more than that of the TaN(N)/TaN film after same plasma treatment time. That is, enhanced nano-crystallization effect on TaN(O)/TaN barrier is found compared to TaN(N)/TaN barrier. The grain size of the TaN film with 30 min O₂ plasma treatment is only ~2 nm, as shown in Fig. 4. It is reported that the nanostructured amorphous diffusion barrier, defined as a very short range order single crystal, is highly attractive due to its relatively higher thermal stability against Cu diffusion.⁹

Chemical bonding states of TaN films were analyzed by XPS. Figure 5 shows the N 1s spectra of TaN films with various N₂ plasma treatments and can give information concerning nitridation effects. The peaks at ~398 eV are ob-

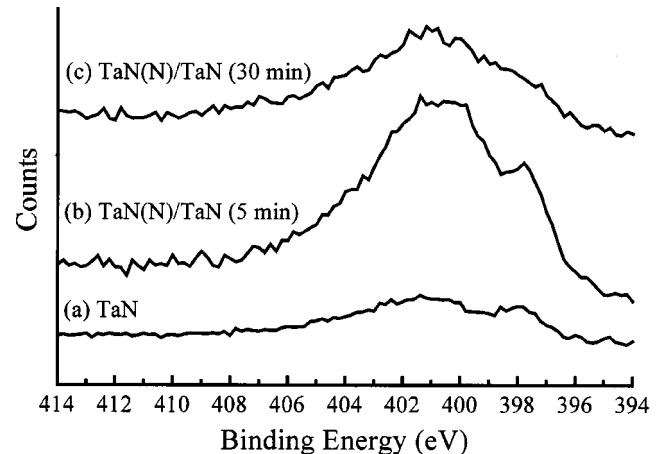


FIG. 5. N 1s XPS spectra obtained from the TaN films with various nitrogen plasma treatments.

TABLE I. Compositions of N₂ plasma-treated TaN (TaN(N)/TaN) films.

Plasma treatment time (min)	Ta (at. %)	N (at. %)
0	59.7	40.3
5	52.1	47.9
15	48.2	52.8
30	34.6	63.4

served in the N 1s spectra for TaN films. It is consistent with the N 1s binding energy of the nitride compound.^{10,11} The presence of the N 1s peak in curve (b) in Fig. 5 clearly shows that the surface is further nitrided by nitrogen plasma. There is another emission peak at ~401 eV observed in N 1s spectrum. This peak at ~401 eV is ascribed to the nitrogen atoms or molecules present in interstitial sites. This kind of nitrogen is also detected in tungsten film prepared by the reduction of WF₆ with N₂ in nitrogen gas.¹⁰ As the N₂ plasma treatment time increases to 30 min, the emission peak at ~401 eV is dominated in the N 1s spectrum. These results indicate that some N atoms do not form strong covalent or ionic bonds with Ta atoms during the plasma nitridation of Ta film. Some of the introduced N atoms segregate at the interstitial sites and grain boundaries in the tantalum film as impurities. Similar results were reported for plasma nitridation of chemical vapor deposited tungsten by Chang *et al.*¹¹ Chemical compositions of untreated and N₂ plasma-treated TaN films were analyzed by XPS and presented in Table I. It is obvious that nitrogen content increases with the increasing nitrogen plasma treatment time. Nitrogen content of untreated TaN film is 40.3 at. %. With 30 min nitrogen plasma treatment, nitrogen content increases to 63.4 at. %. Figure 6 shows O 1s XPS spectra of TaN films after O₂ plasma treatments for various durations. Oxygen bonding states are increasingly observed with increasing O₂ plasma treatment, as shown in Fig. 6. The position of the O 1s level is not clearly observed for the 5 min O₂ plasma-treated TaN film. The peak of binding energy corresponding to oxygen bonding can be

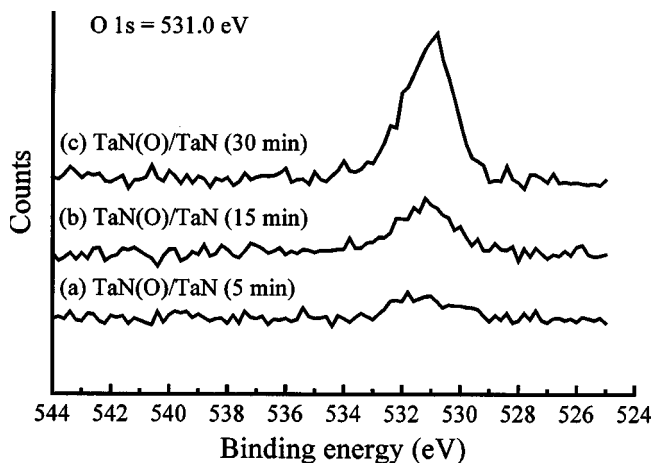


FIG. 6. O 1s XPS spectra obtained from the TaN films with various oxygen plasma treatments.

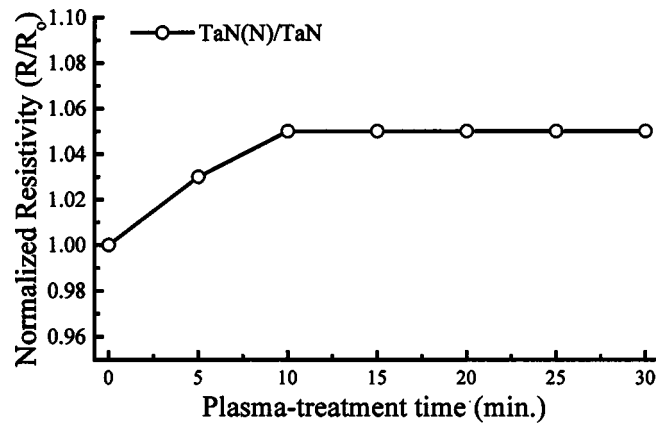


FIG. 7. Normalized resistivity of TaN(N)/TaN film as a function of plasma treatment time.

observed for the TaN films with 15 min O₂ plasma treatments. Ta–N–O compound is believed to form after the O₂ plasma treatment.

Normalized resistivity of TaN(N)/TaN film as a function of plasma treatment time is plotted in Fig. 7. The resistivity of untreated TaN film is set to be one. The normalized resistivity initially increases with increasing N₂ plasma treatment time and then becomes constant after 10 min plasma treatment as shown in Fig. 7. Nitridation and nano-crystallization effects are believed to result in increase in the resistivity. In our previous study, it was found that sputtered Ta films had a resistivity of 197 $\mu\Omega$ cm and resistivity of the reactively sputtered TaN film would initially decrease to 159 $\mu\Omega$ cm and then increase to higher than 3500 $\mu\Omega$ cm as nitrogen flow ratio increased during reactive sputtering.⁵ As mentioned in experimental details, TaN films with low resistivity of 159 $\mu\Omega$ cm were prepared and used in this work. It is expected that resistivity of TaN(N)/TaN film would increase because a high-resistance surface layer forms and thus the effective thickness of the TaN film with low resistivity reduces. However, the increase of the resistivity is slight (~6%) and the resistivity is about 170 $\mu\Omega$ cm which is much lower than that of the reactively sputtered TaN film with high nitrogen concentration. Though the detailed mechanisms are needed to be further investigated, the resistivity becomes constant probably because the thickness of the surface layer saturates after 10 min N₂ plasma treatment. Normalized resistivity of TaN(O)/TaN film is higher than that of TaN(N)/TaN film. The increase of the resistivity may be due to the formation of high-resistance Ta–O compound. However, the resistivity of TaN(O)/TaN film is still much lower than that of the reactively sputtered TaN film with high nitrogen concentration.

B. Thermal stability of Cu/barrier/Si system

Cu/barrier/Si systems annealed at various temperatures were characterized by sheet resistance. Figure 8 shows variation of sheet resistance of Cu/barrier/Si as a function of annealing temperature. The variation of sheet resistance is designed as the ratio of ($R-R_0$) to R_0 , where R_0 and R denote

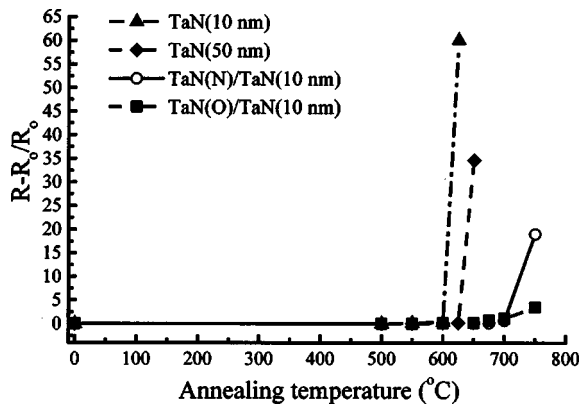
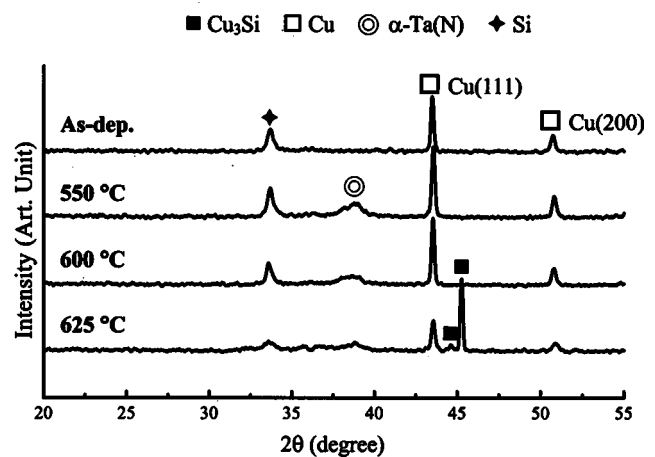


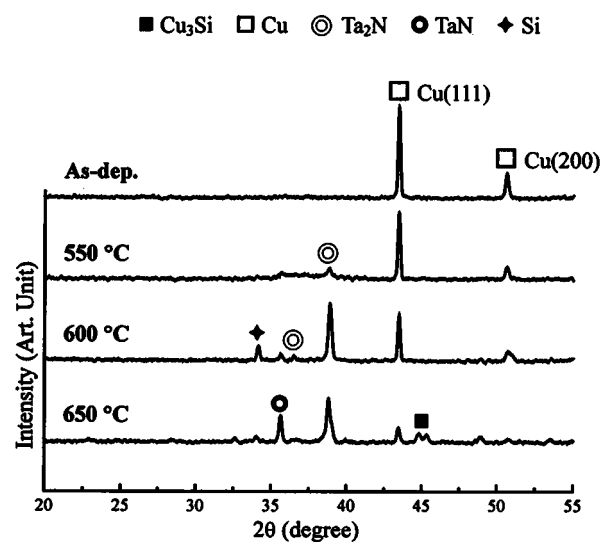
Fig. 8. Variation of sheet resistance of Cu/barrier/Si system as a function of annealing temperature.

the sheet resistance of as-deposited and annealed sample, respectively. The results reflect interactions between Cu and Si indirectly. The data mainly indicate changes in the thickness or resistivity of the unreacted copper layer, since the resistance of the barrier layer and reaction products are expected to be much larger than that of Cu. An abrupt increase of sheet resistance occurs and the surfaces become gray for the samples with sputtered TaN(10 nm) and TaN(50 nm) barriers after annealing at 625 and 650 °C, respectively. This implies that Cu has diffused into silicon substrate. Tsai *et al.* reported similar results. An obvious increase was found for the sheet resistance of the Cu/physical vapor deposition TaN(60 nm)/Si system after annealing at 650 °C for 30 min.¹² Sheet resistance of the samples with 30 min plasma-treated TaN barrier layers only increases a little after annealing at 750 °C for 1 h, as shown in Fig. 8. It is obvious that thermal stability of TaN barrier can be increased by plasma treatment.

Figure 9 shows the XRD spectra for Cu/TaN/Si samples after annealing at various temperatures for 1 h. Figure 9(a) clearly shows the formation of copper silicide (Cu_3Si) for the Cu/TaN(10 nm)/Si sample after annealing at 625 °C. The results are consistent with the abrupt increase in the sheet resistance as shown in Fig. 8. Strong Ta_2N and TaN peaks are found for the samples with 50 nm TaN barrier layers after annealing at higher than 600 °C. The peaks of Cu_3Si are observed after annealing at 650 °C, as shown in Fig. 9(b). Failure of barrier layer is attributed to enhanced crystallization of the TaN film after high-temperature annealing. On the other hand, the peak of copper silicide is not observed for the sample with 10 nm TaN(N)/TaN or TaN(O)/TaN barrier layer annealed at 700 °C, as shown in Fig. 10. It is obvious that plasma treated TaN barrier possesses higher thermal stability and can impede Cu diffusion into the Si substrate. Additional results have been obtained in AES depth profiles. Figure 11 shows the AES depth profiles of Cu/TaN(O)/TaN/Si after annealing at 700 °C for 1 h. As is expected from results of XRD and sheet resistance, no significant interdiffusion is observed between Cu and Si. It reveals that plasma-treated TaN barrier possesses excellent barrier performance.



(a)



(b)

Fig. 9. XRD spectra of Cu/TaN/Si systems after annealing at various temperatures for 1 h. (a) 10 nm. (b) 50 nm.

SEM was used to examine the surface morphologies after thermal annealing for further analyzing thermal stability. Protrusions or precipitates are observed on the surface after annealing at the temperature that an abrupt increase of sheet resistance occurs. Figure 12 shows the SEM micrograph and chemical composition analyses of the sample with TaN(O)/TaN barrier film after annealing at 750 °C for 1 h. Figure 12(a) shows surface morphology of silicon substrate after copper and tantalum nitride are stripped. It reveals local defect sites, as denoted as region B in Fig. 12(a). EDS is further employed to analyze the chemical compositions in region B. The concentrations of copper and silicon are 74.23 and 25.77 at. %, respectively. It is evident that the ratio of Cu to Si approximates 3 in region B. Distributions of Cu and Si in region B are further analyzed by mapping. Copper is uniformly distributed as shown in Fig. 12(c). Figure 12(d) shows the mapping of silicon. Less silicon is observed in region B. It reveals that copper has already penetrated the barrier film into silicon substrate after annealing at 750 °C

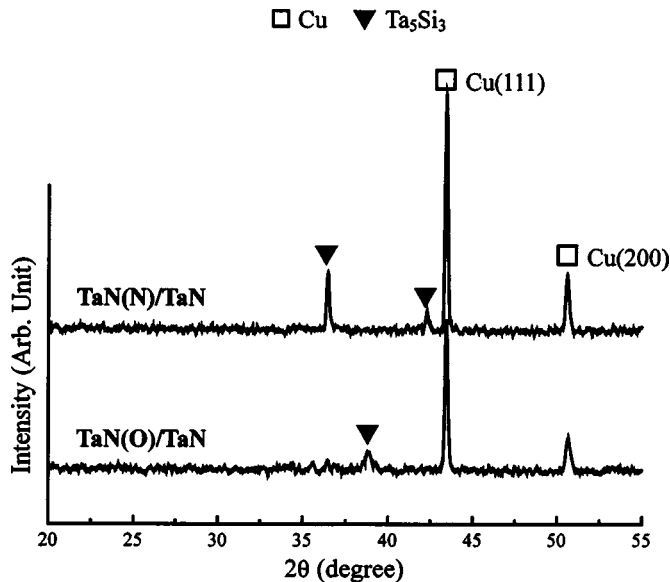


FIG. 10. XRD spectra of Cu/TaN(N)/TaN(10 nm)/Si and Cu/TaN(O)/TaN(10 nm)/Si systems after annealing at 700 °C for 1 h.

and copper silicide forms as Cu_3Si . From the results of sheet resistance and SEM, the abrupt increase of resistance is ascribed to the formation of Cu_3Si compound in Si substrate. The results of SEM and EDS are in good agreement with the sheet resistance.

C. Electrical properties of Cu/barrier/ n^+ - p diodes

Barrier capabilities of TaN(10 nm), TaN(50 nm), TaN(N)/TaN(10 nm), and TaN(O)/TaN(10 nm) films are further investigated by evaluating the integrity of Cu/barrier/ n^+ - p junction diodes after stressing by thermal annealing. Figure 13 illustrates the statistical distributions of reverse biased leakage current densities measured at -5 V for Cu/barrier/ n^+ - p junction diodes annealed at various temperatures. With a failure criterion of 10^{-6} A/cm², the Cu/TaN(10 nm)/ n^+ - p diodes remain stable after annealing at temperatures up to 500 °C but suffer degradation at 525 °C as shown in Fig. 13(a). Figure 13(b) shows the statistical distributions of reverse biased leakage current densities for the Cu/TaN(50 nm)/ n^+ - p junction diodes annealed at various temperatures. The diodes remain stable after annealing at temperature up to

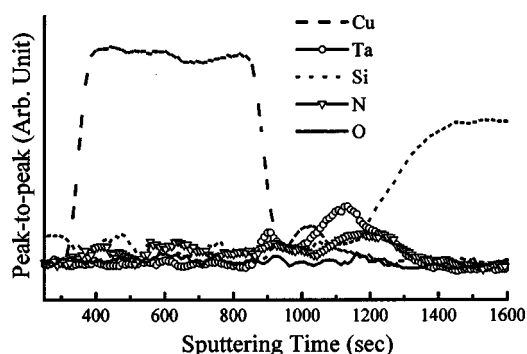


FIG. 11. AES compositional depth profiles of Cu/TaN(O)/TaN/Si after annealing at 700 °C.

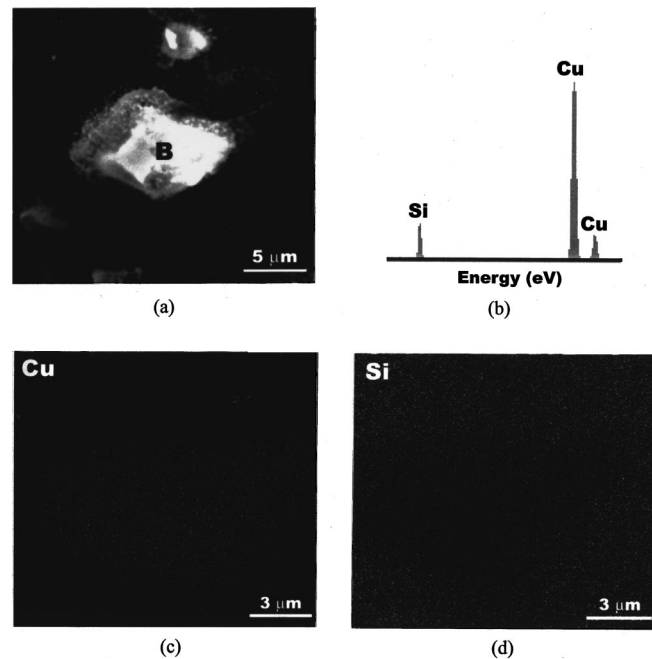


FIG. 12. (a) SEM micrograph of Cu/TaN(O)/TaN/Si sample annealed at 750 °C for 1 h. (b) EDS spectrum obtained from region B in Fig. 12(a). Mapping analyses for (c) Cu and (d) Si in region B.

550 °C for the diodes with 50 nm TaN barriers. Failure of the diode is observed after annealing at 575 °C. Thermal stability of the Cu/TaN/ n^+ - p junction diode is found to be dependent on the thickness of the barrier layer. As thickness of the TaN barrier layer increases from 10 to 50 nm, the failure temperature is increased ~ 50 °C. However, as the devices become smaller and dimensions decline below 180 nm, it becomes inappropriate to use a barrier layer thicker than 30 nm. The barrier thickness should be reduced to lower the resistance of the total line interconnect and/or via. As mentioned previously, N_2 and O_2 plasma treatments are used to improve barrier capabilities of ultrathin TaN layers (10 nm). The Cu/TaN(N)/TaN/ n^+ - p diodes remain stable after annealing at 550 °C, as shown in Fig. 13(c). Moreover, most Cu/TaN(N)/TaN/ n^+ - p diodes have low junction leakage currents even after thermal stressing at 650 °C. The TaN(N)/TaN films possess much better barrier performance than untreated TaN films. Figure 13(d) shows the statistical distributions of reverse biased leakage current densities for Cu/TaN(O)/TaN(10 nm)/ n^+ - p junction diodes annealed at various temperatures. Highly improved barrier capability against Cu diffusion is observed since low leakage currents are obtained for Cu/TaN(O)/TaN(10 nm)/ n^+ - p junction diodes even after annealing at 650 °C for 1 h. Improved barrier performance is attributed to nano-crystallization and stuffing effects due to the reactions and bombardments of energetic radicals and ions during plasma treatment. It is reported that the microstructure within the barrier layer strongly affects the barrier performance because Cu diffuses through fast diffusion paths such as grain boundaries within the barrier layer.^{5,6,13} The thin amorphous TaN_x and TaN_xO_y layers form on the surface of the TaN films after nitrogen and oxygen plasma treat-

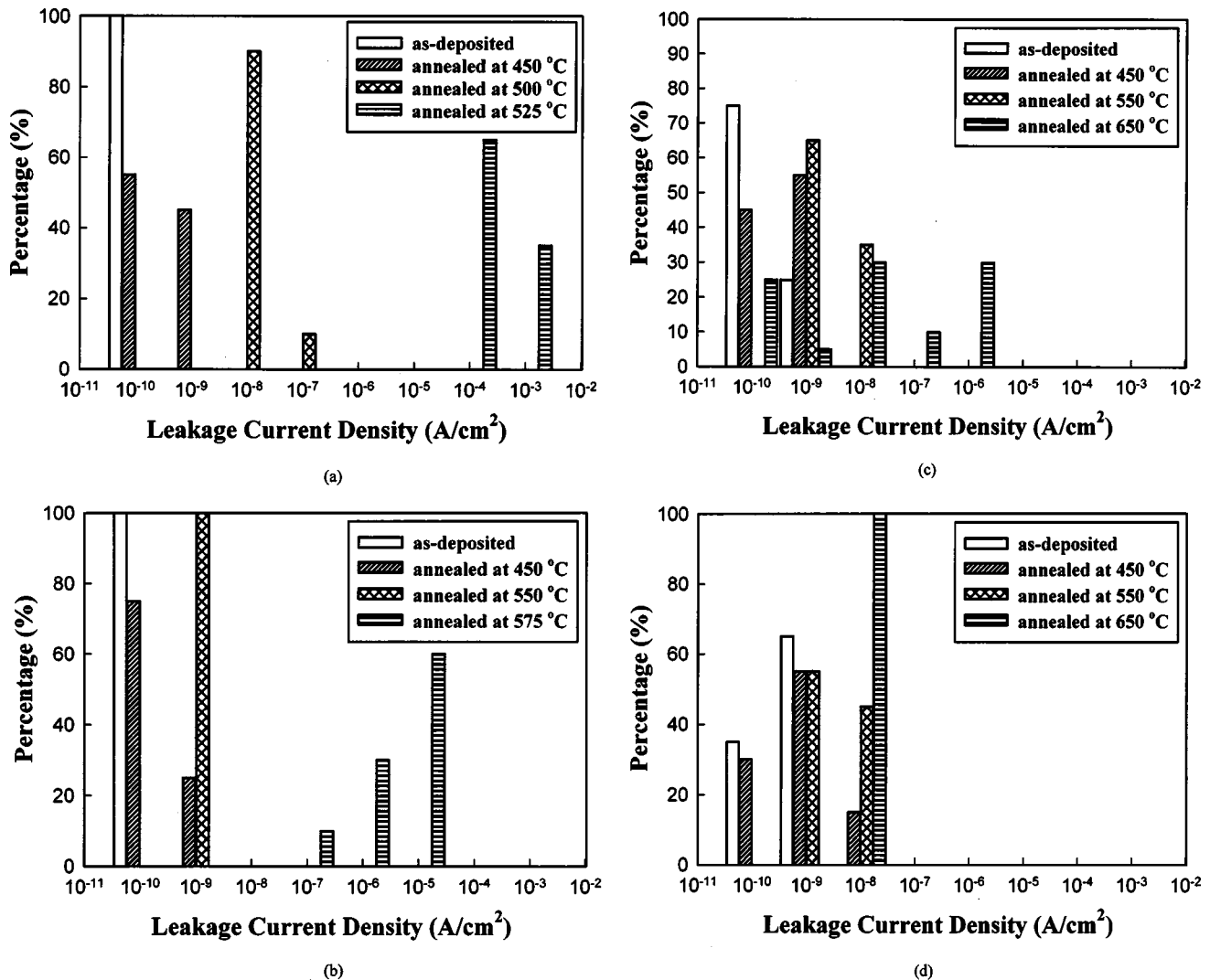


FIG. 13. Statistical distributions of reverse-biased leakage current densities for (a) Cu/TaN(10 nm)/n⁺-p, (b) Cu/TaN(50 nm)/n⁺-p, (c) Cu/TaN(N)/TaN(10 nm)/n⁺-p, and (d) Cu/TaN(O)/TaN(10 nm)/n⁺-p junction diodes annealed at various temperatures for 1 h.

ments. Amorphous diffusion barrier is more effective for preventing Cu diffusion than the polycrystalline barrier since the amorphous film does not have large-angle grain boundaries where most of the atomic diffusion typically occurs.⁹ More improved barrier performance is found for TaN(O)/TaN barrier due to enhanced nano-crystallization effect compared to TaN(N)/TaN barriers.

IV. CONCLUSION

The effectiveness of tantalum nitride with N₂ or O₂ plasma treatment as a diffusion barrier between copper and silicon has been investigated. An amorphous layer is found to form on the surface of the TaN film after the plasma treatment. The oxygen and nitrogen bonding states are observed for O₂ and N₂ plasma-treated TaN films. Thermal stabilities of plasma-treated barriers TaN(N)/TaN and TaN(O)/TaN are better than those of untreated barriers TaN(10 nm) and TaN(50 nm). Nano-crystallization and stuffing effects as well as nitridation and oxidation are observed. A new amorphous layer can be induced on the surface of the TaN barrier with

the reactions and bombardments of nitrogen or oxygen radicals and ions. The barrier performance of the TaN film is improved apparently after plasma treatment. The Cu/TaN(N)/TaN(10 nm)/Si and Cu/TaN(O)/TaN(10 nm)/Si contact systems remain stable after annealing at 700 °C for 1 h. Thermal stability and electrical integrity of Cu/TaN/n⁺-p junction diodes are enhanced by plasma treatment. The failure temperature of the sample with plasma-treated TaN barrier is about 150 °C higher than that of the sample with untreated TaN barrier. Nano-crystallization and stuffing effects of plasma treatments are believed to impede Cu diffusion into the Si substrate and hence improve the barrier performance. More improved barrier performance is found for TaN(O)/TaN barrier due to enhanced nano-crystallization effect compared to TaN(N)/TaN barrier.

ACKNOWLEDGMENT

The authors would like to thank the National Science Council of the Republic of China for financially supporting

this research under Contract Nos. NSC 90-2215-E-317-005 and NSC 91-2722-2317-200.

- ¹Y. J. Lee, B. S. Suh, M. S. Kwon, and C. O. Park, *J. Appl. Phys.* **85**, 1927 (1999).
- ²Y. L. Chin, B. S. Chiou, and W. F. Wu, *Jpn. J. Appl. Phys., Part 1* **39**, 6708 (2000).
- ³T. Kouno, H. Niwa, and M. Yamada, *J. Electrochem. Soc.* **145**, 2164 (1998).
- ⁴M. Uekubo, T. Oku, K. Nii, M. Murakami, K. Takahiro, S. Yamaguchi, T. Nakano, and T. Ohta, *Thin Solid Films* **286**, 170 (1996).
- ⁵W. L. Yang, W. F. Wu, D. G. Liu, C. C. Wu, and K. L. Ou, *Solid-State Electron.* **45**, 149 (2001).
- ⁶K. H. Min, K. C. Chun, and K. B. Kim, *J. Vac. Sci. Technol. B* **14**, 3263 (1996).
- ⁷M. Stavrev, D. Fischer, C. Wenzel, K. Drescher, and N. Mattern, *Thin Solid Films* **307**, 79 (1997).
- ⁸T. Oku, E. Kawakami, M. Uekubo, K. Takahiro, S. Yamaguchi, M. Murakami, S. Yamaguchi, and M. Murakami, *Appl. Surf. Sci.* **99**, 265 (1996).
- ⁹D. J. Kim, Y. T. Kim, and J. W. Park, *J. Appl. Phys.* **82**, 4847 (1997).
- ¹⁰T. Nakajima, K. Watanabe, and N. Watanabe, *J. Electrochem. Soc.* **134**, 3175 (1987).
- ¹¹K. M. Chang, T. H. Yeh, I. C. Deng, and C. W. Shih, *J. Appl. Phys.* **82**, 1469 (1997).
- ¹²M. H. Tsai, S. C. Sun, C. E. Tsai, S. H. Chuang, and H. T. Chiu, *J. Appl. Phys.* **79**, 6932 (1996).
- ¹³G. S. Chen and S. T. Chen, *J. Appl. Phys.* **87**, 8473 (2000).